Supplementary material

Cells Have the Ability to Break and Chemically Modify GaP(As) Nanowires

Stanislav V Shmakov, Zlata P Sosnovitskaia, Ekaterina A Makhneva, Maria A Anikina, Alexey Kuznetsov, Valeriy M Kondratev, Nikita Solomonov, Vitali M Boitsov, Vladimir V Fedorov, Ivan S Mukhin, Anton S Bukatin* and Alexey D Bolshakov**

Nanowires surface density

Plane view SEM image in **Figure S1** displaying vertical GaP(As) NWs was utilized to quantitatively estimate their surface density. The calculated density was estimated at 1 μm^{-2}. With a cell area of 400 μm^2, it was determined that there are approximately 400 NWs beneath each cell.

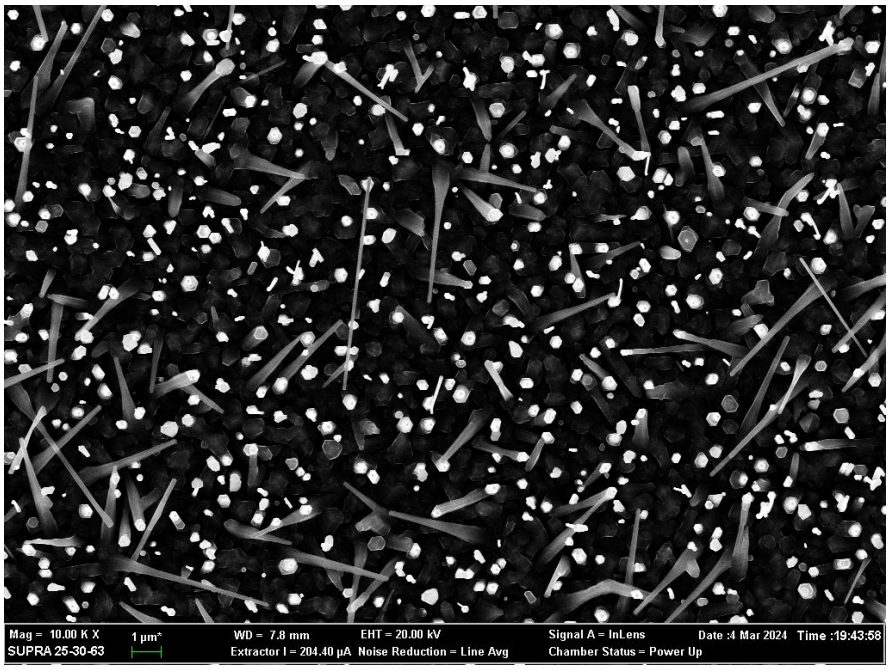

Figure S1. Plane view SEM image of the GaP(As) NWs array.

Additional luminescence MosaiX images

Here we present the obtained large representative 25 MosaiX images (500µm·500µm each) of the cells cultivated on control Si surface and on vertical GaP(As) nanowires (NWs), see **Figure S2**.

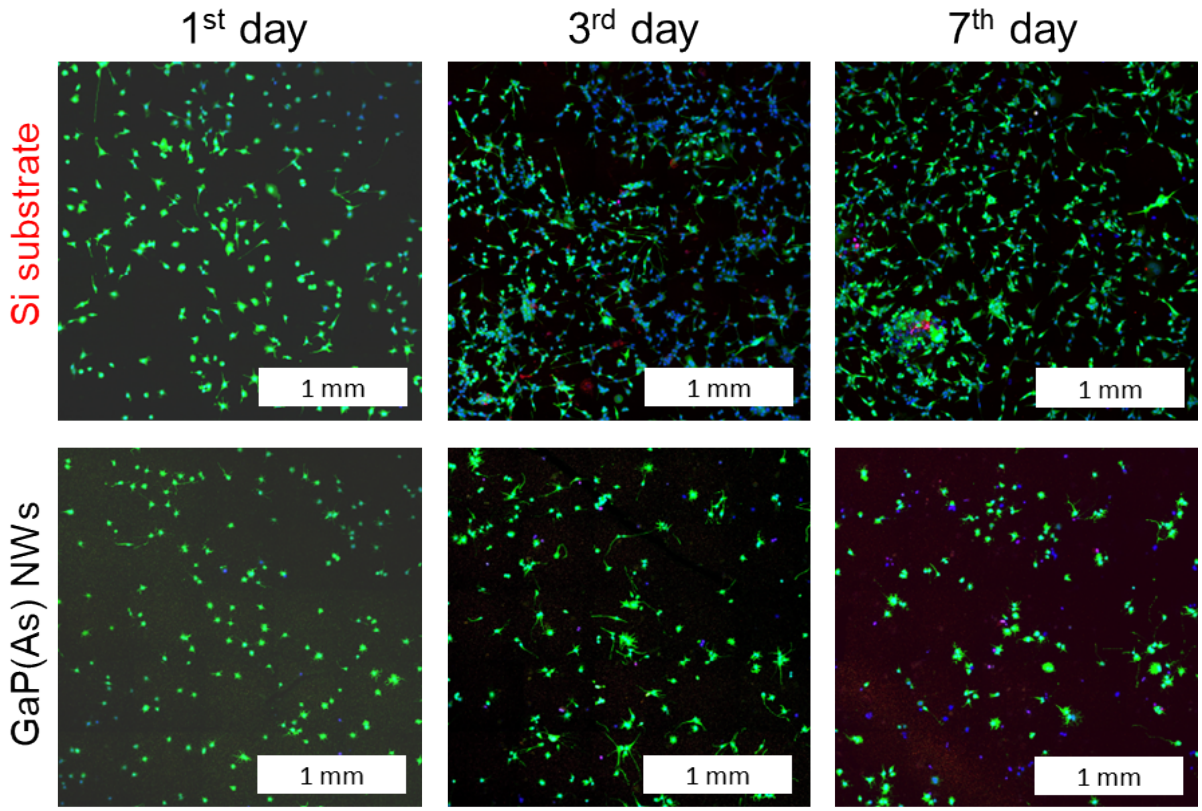

Figure S2. 5x5 MosaiX images corresponding to the 1st, 3rd, and 7th days of incubation on reference Si substrate and on GaP(As) NWs.

Morphology change and cell death

Mean area of a cell cultured on GaP(As) NWs was compared with the corresponding value for a cell on control Si wafer. The analysis of optical images shows that the average size of cells in the control sample does not change significantly with the cultivation period. At the same time, the cells grown on the surface of vertical NWs show a tendency to increase the area by 50% compared to the control sample (see **Figure S3** below) due to the formation of pseudopodia. Thus, the measurement of cell area allows to numerically characterize the change in the morphology of the cells cultured on the NWs.

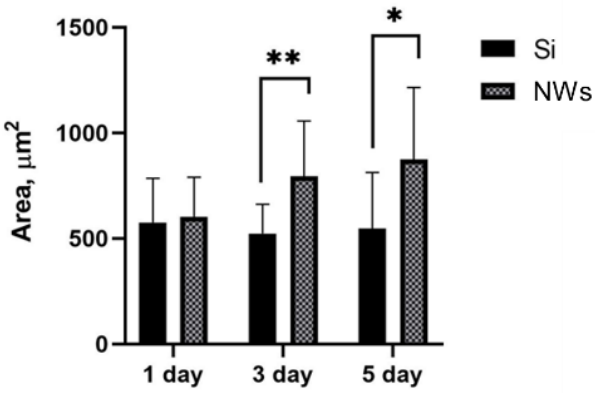

Figure S3. Dynamics of the mean cell area for the control sample and cells cultivated on GaP(As) NWs.

We investigated the type of cell death for various types of NWs with an aid of flow cytometry using standard DAPI/Annexin V-FITC staining of CT26 cells cultured on the surface of 2 μm long GaAs NWs, 4 μm and 8 μm long GaP NWs. The obtained data,

presented in **Figure S4** shows that a substantial fraction of cells underwent membrane inversion, indicating a significant proportion of early and late apoptosis in the population. Although the flower-like morphology of cells does resemble the changes that occur during the late phase of apoptosis, the presence of such morphological changes is more prominent when the cells are cultured on GaP/GaPAs NWs, while the membrane inversion characteristic of apoptosis is observed regardless of the NW composition. Thus, we conclude that these changes in morphology are not directly related to the onset of apoptosis.

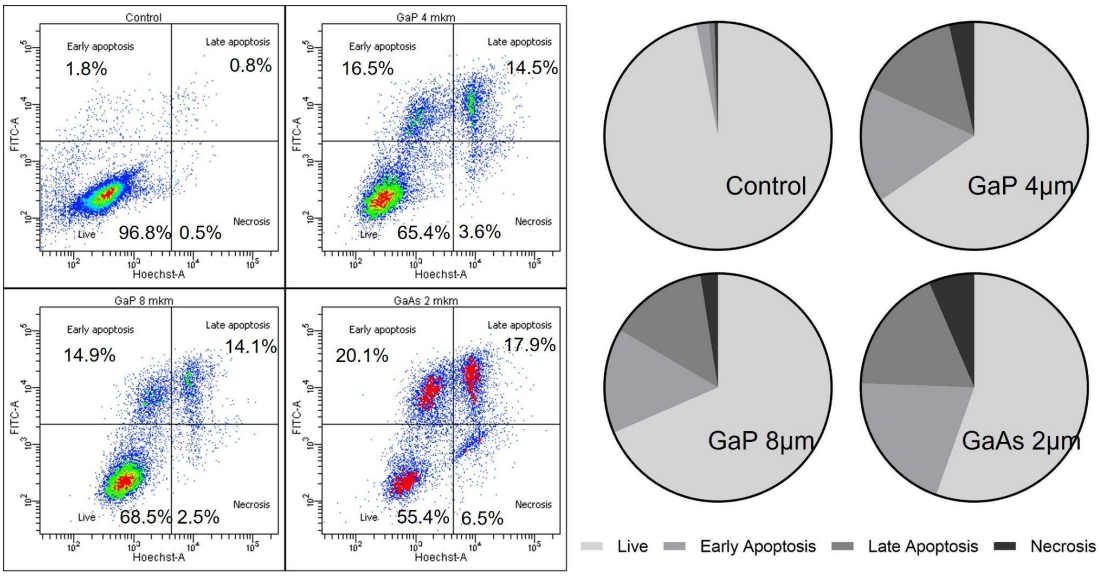

Figure S4. Flow cytometry results of the type of cell death study using DAPI/Annexin V-FITC staining of CT26 cells cultured on the surface of control Si substrate, 2 μm long GaAs NWs, 4 μm and 8 μm long GaP NWs.

Images of vertical NWs

Figure S5 depicts images of GaP and GaAs NWs used in the cultivation experiments.

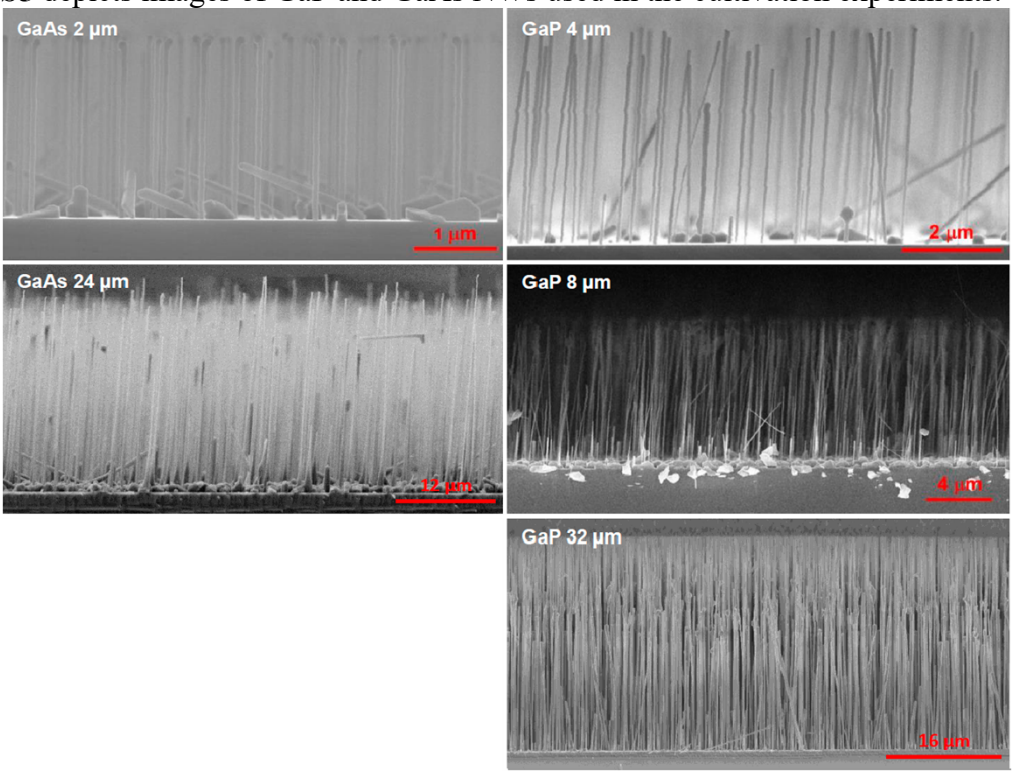

Figure S5. SEM images of GaP and GaAs vertical NWs used in the cultivation experiments.

Cell cycle phases

Distribution of CT26 cells by cell cycle phases was studied using flow cytometry. For the experiment we cultured the cells on the control Si substrate and 3 types of NWs: 4 μm and 8 μm long vertical GaP NWs, 2 μm GaAs NWs. Interestingly, our findings presented in **Figure S6** suggest that cultivation of cells on NWs does not significantly alter the distribution of cells by the cycle phases. The ratio between G0/G1:S:G2/M for the control Si sample is 3.2:1.3:1, for 4 μm vertical GaP NWs 3.9:1.6:1, for 8 μm GaP NWs 3.1:1.2:1 and for 2 μm GaAs NWs 3.6:1.2:1. Thus, the ratio between the cell cycle phases is practically unchanged, apart from the appearance of a significant number of cells in the SubG phase in the case of 8 μm GaP NWs. The preservation of the ratios of cell cycle phases may manifest normal cell division rate during the cell cultivation on NWs.

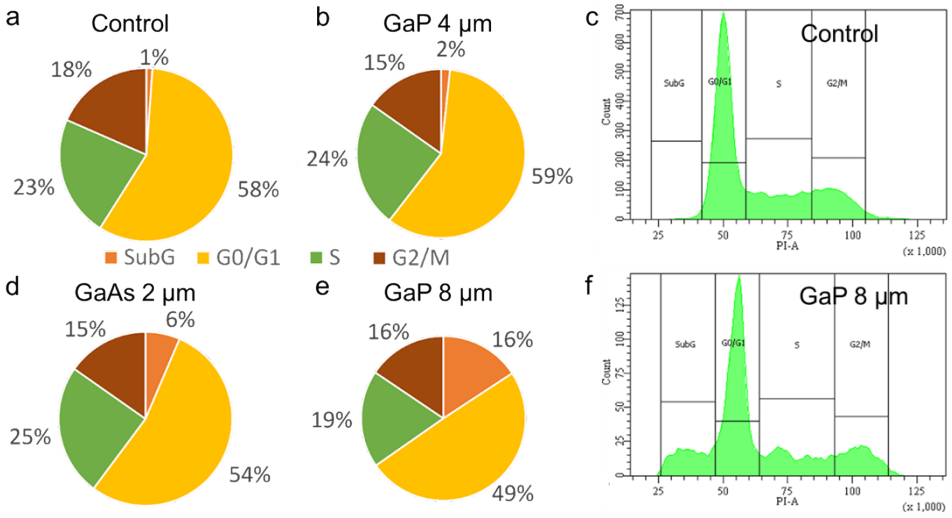

Figure S6. Distribution of CT26 cells by cell cycle phases: a) control sample (cells cultured on Si substrate), b) cells cultured on vertical 4 μm long GaP NWs, c) corresponding flow cytometry graph of the cell cycle phases (control sample), d) cells cultured on vertical 2 μm long GaAs NWs, e) cells on vertical 8 μm long GaP NWs, f) corresponding flow cytometry graph of the cell cycle phases (cells on 8 μm GaP NWs).

Proliferation statistics

Let us now analyze statistics of proliferation of the CT26-EGFP cells (see **Figure S7**) when cultured on NWs of different morphology and composition (as presented in paragraph 2.2, main text). In 24h after the cell spreading, a significant difference with the control sample (16.4±7.5 cells per frame (cpf)) is observed only in the case of 32 μm long GaP (4.8±2.7 cpf), 2 μm GaAs (6.5± 4.5) and 24 μm GaAs (1.6±0.6 cpf) NWs. In the case of 24 μm GaAs NWs there is an almost complete absence of cells. In the case of the longest 32μm GaP NWs, only few cells were observed. Thus, we can conclude that the NWs composition is a critical parameter for the cell growth, since cell proliferation on longer GaP NWs is suppressed but possible, while in the case of shorter GaAs NWs cells die intensively 48 hours after the spreading. When cells were dispersed on 4 and 8.5 μm long GaP NWs, on the first day of the experiment there was no significant difference with the control sample, which indicates the absence of acute toxicity and good cell adhesion. 48 hours after the dispersal, the number of cells on 4 μm long GaP NWs continues to increase, and is about 30% of the control sample on days 4-5. In the case of 8.5 μm long GaP NWs on day 3 the number of cells coincides with the number of cells on 4 μm long GaP NWs, however, on days 4 and 5 the number of cells on the surface significantly decreases down to 5.2±5.5 cpf. Such a decay may indicate a

significant heterogeneity of the surface morphology. In the case of GaAs NWs with a length of 2 μm, a significant decrease in the number of cells is observed starting from the first day. After 1 day incubation the number of cells was 6.4 ±4.4 cpf. Up to 4th day, the number of cells slowly increases and reaches 22.6±17.4 cpf, which is approximately 15% of the cells cultured on the silica surface and decreases to 16.3±10.1 cpf on the next day. Comparing these results with the data of the cell cycle phases, we conclude that GaP NWs with characteristic lengths of 4 and 8.5 μm, do not induce changes in proliferation rate, although they do affect the cell viability. Thus, such NWs are considered as good candidates for studying e.g. transfection. The results are averaged of 3 replicates in each experiment, given as the mean ± SD values. ** $p \leq 0.01$ ****$p \leq 0.0001$.

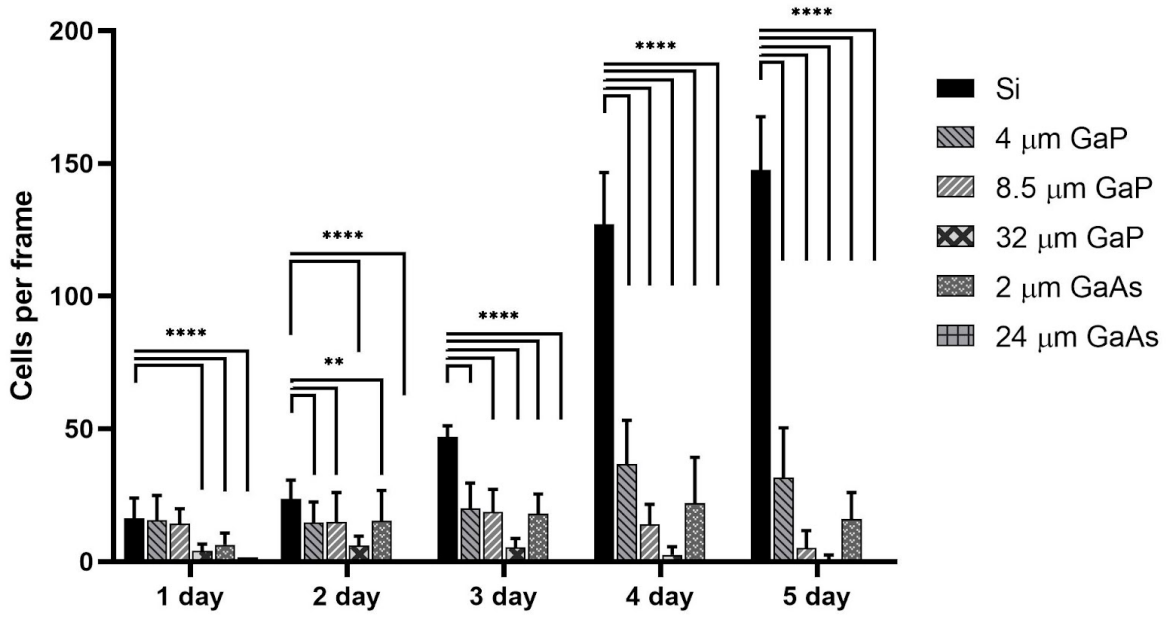

Figure S7. CT26-EGFP proliferation on vertical NWs: GaP (4, 8.5 and 32 μm long) and GaAs (2 and 24 μm long), and on control Si wafer.

Statistical analysis of the transfection data

Statistical processing of the experimental data on transfection efficiency of the cells cultivated on 8 μm long GaP NWs and control Si wafer was performed using GraphPad Prism 8. The data of three independent experiments were used for measuring the mean transfection efficiency ± standard deviation that were compared using the Student's *t*-test. When cultured on NWs, the number of transfected HeLa cells showing fluorescence in cytoplasm was 52.57±17.82%. While in case of cultivation on Si wafer, the number of the transfected cells was 4.12±3.68%, P value<0.0001. Differences among groups were considered significant at $p \leq 0.05$.

CT26 culture transfection

We carried out transfection of the CT26 cell line similarly to the protocol used with HeLa cells on 4 μm long GaP NWs. Experiments unveiled that unlike with the HeLa line, the transfection efficiency of CT26 was highly non-uniform and dependent on the specific substrate site. We obtained quite high transfection efficiency in some areas (shown in **Figure S8**).

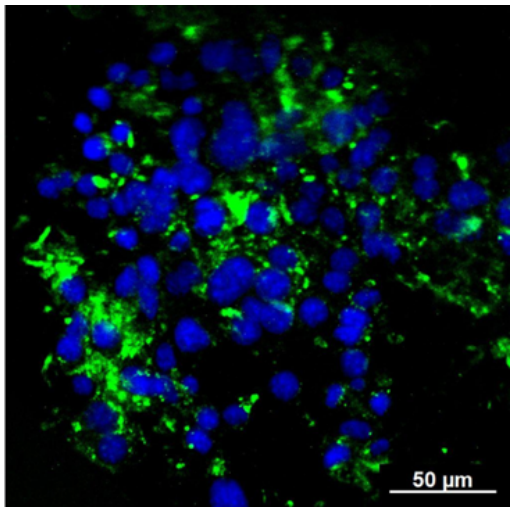

Figure S8. Fluorescence image of the CT26 cells cultivated on vertical GaP NWs and transfected with pMaxGFP plasmid.

HEK culture transfection

One of the most convenient culture for studying transfection and optimizing corresponding protocols is HEK293T. Cultivation of these cells have been performed on vertical GaP NWs followed by transfection with pmaxGFP, however, showing low transfection efficiency. This can be explained by the peculiarities of the culture growth: HEK293T tend to form "islands", which seems to be even more pronounced when cultured on the surface of the NWs suppressing the transfection. **Figure S9** depicts fluorescence image of the transfected cells.

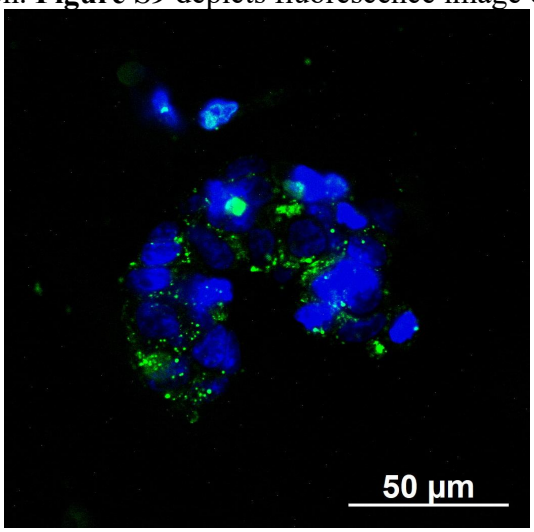

Figure S9. Fluorescence image of the HEK293T cells cultivated on vertical GaP NWs and transfected with pmaxGFP plasmid.

PI control

Figure S10 shows a positive control of HeLa cells staining with PI dye. The staining was performed using the standard protocol for immunocytochemical staining of cells. The culture was fixed with 4% PFA solution on PBS for 10 minutes at room temperature. Then washed three times with PBS, permeabilized with 0.01% Triton X-100 for 10 minutes at room temperature, and again washed three times with PBS. After that, cells were stained with PI and analyzed with fluorescence microscopy.

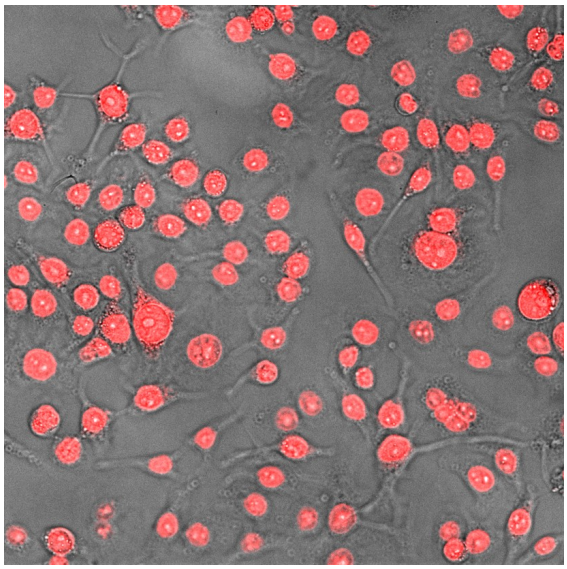

Figure S10. Fluorescence optical image of the HeLa cells stained with PI.

Fluorescence microscopy artefacts

Unfortunately, our fluorescence microscope optical scheme has an artefact that manifests itself in a green channel. These spots can be seen in all the images when excited with the 488 nm laser. To demonstrate the effect, we supply a blank photo (image taken without a sample, **Figure S11**).

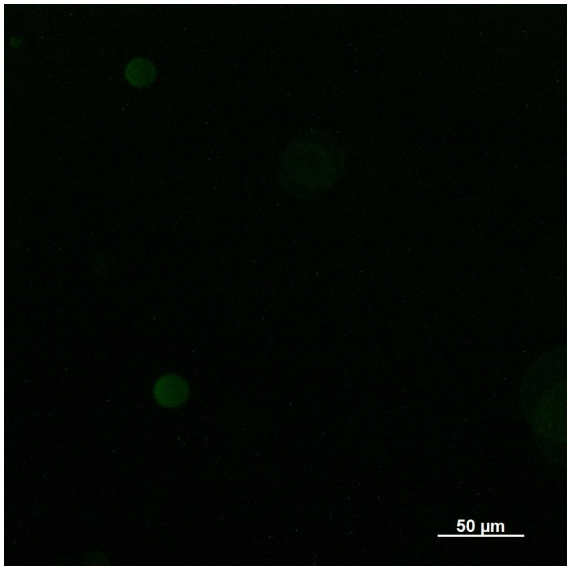

Figure S11. Blanck image collected in the green channel of fluorescence microscope.

Oxidation of GaPAs ternary insertions

In order to gain insight into the oxidation process of GaPAs inserts resulting in the red spectral shift of the NWs' luminescence, we performed additional experiments. We treated a sample containing as-grown vertical GaP(As) NWs with a 3% aqueous solution of hydrogen peroxide for 30 minutes. The sample was then analyzed using luminescence microscopy. We compared the results with two reference samples (reported in Figure 4, main text). Images of the reference GaP(As) NWs after 1day of CT 26 incubation, 5 days of

incubation and of the extra sample subjected to peroxide treatment are presented in **Figures S12**a, S12b and S12c, correspondingly. In the images green false color represents green light of the cells collected with 527/54 nm channel. Blue false color - light collected with 629/62 nm channel and visualizes short range NWs' luminescence. Red color - light collected with 690/50 nm channel, long range NWs' luminescence. The results demonstrate a similar effect of the CT26 cells incubation and peroxide treatment on the NWs' luminescence. In both cases NWs undergo a red shift of the luminescence.

To delve deeper into these findings, we utilized Energy-dispersive X-ray (EDX) spectroscopy of the NWs treated with peroxide. The spectra displayed in Figure S12d reveal a simultaneous increase in oxygen content and a decrease in arsenic content. These results support the hypothesis of oxidation and substitution of arsenic atoms by oxygen in GaP(As) NWs under the influence of the cells.

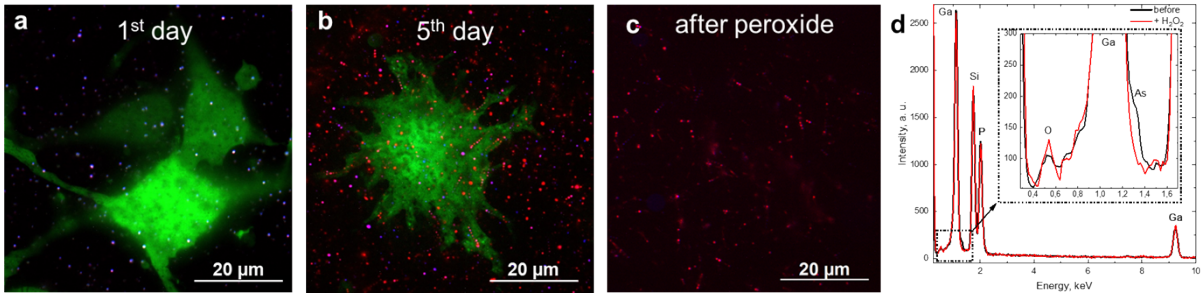

Figure S12. Effect of CT26 cells and hydrogen peroxide treatment on luminescence of GaP(As) NWs. Confocal fluorescence images illumination - 488 nm, collection through 527/54 nm (green false color), 629/62 nm (blue dots) and 690/50 nm (red dots) filters: a) cells cultivated on vertical GaP(As) NWs for 1 day, b) 5 days of incubation, c) as-grown vertical GaP(As) NWs after peroxide treatment. d) EDX spectra of the GaPAs inserts before (black curve) and after (red curve) the peroxide treatment.

To prove that the spectrum shift is not related to the fluorescent GFP protein and even not specific to CT26 line, we performed a similar experiment with incubation of NWs with lysate of HeLa cells. The obtained data demonstrate that we observe a similar change in the NWs' fluorescence depicted in fluorescence image in **Figure S13**.

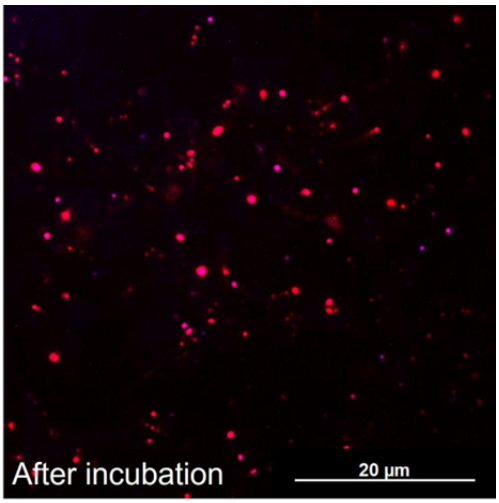

Figure S13. Fluorescence image of the vertical GaP(As) NWs after the addition of HeLa cells lysate.

Flow cytometry of cells cultured on GaP(As) nanowires

To support the hypothesis of the NWs internalization by the cells two samples with CT26 cells in a plate (control) and on GaP(As) NWs were cultured for 3 days The cells were then subjected to flow cytometry. The histograms of fluorescence intensity distribution in the PerCP-CY5 channel (excitation – 488 nm, collection through 695/40 nm filter) are presented in **Figure S14**. The results show a clear difference between the control sample and the cells cultivated on luminescent nanowires. We observed the emergence of a distinct P6 subpopulation with more pronounced red fluorescence in cells cultivated on NWs, accounting for 26% of the total cell population compared to only 4% in the control group. The significant increase in the P6 subpopulation with enhanced fluorescence intensity provides compelling evidence of nanowire association with the cells.

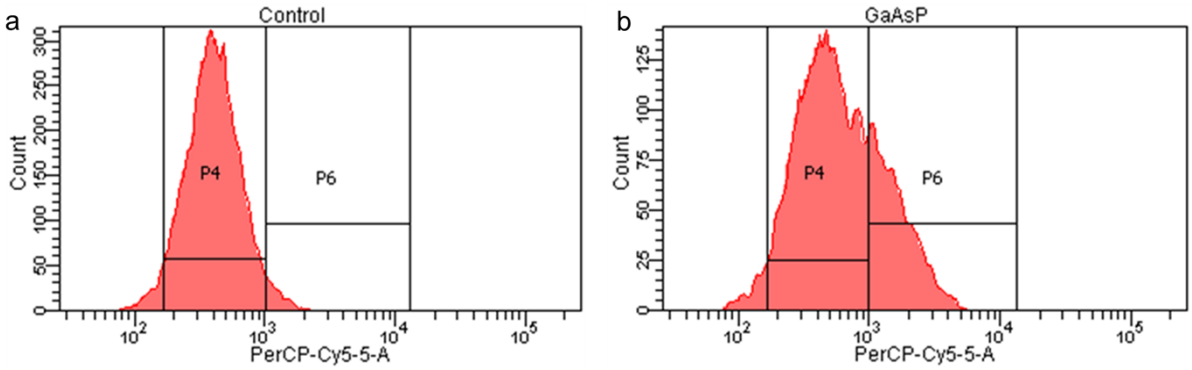

Figure S14. Flow cytometry results, NWs association with the cells. Fluorescence intensity distribution of CT26 cells in the PerCP-CY5 channel: a) control sample. b) cells cultured on vertical GaP(As) NWs for 3 days.

Cell forces

Following [1] we consider the bending action of the cell on NW as a concentrated force F applied to the nanostructure (see schematic on insert in Figure 5e, main text). Using the elastic approximation, this force and the resulting NW tip displacement (deflection) can be calculated for a specific elastic strain. According to the previous studies, elastic limit of GaP NWs is 3% at the least. [2,3] This value can be used to estimate the mechanical strength of the nanostructure. [4] The GaPAs inserts cause additional strain at the heterointerfaces due to the lattice mismatch between GaP and GaPAs with magnitude not exceeding 2%. While this increased strain at the heterointerfaces could potentially impact the outcomes, the overall force order is expected to remain consistent.. The cell action on a NW can be considered as a planar transverse bending of the nanoscale beam, which leads to the occurrence of transverse forces Q and bending moment M. According to the strength of materials theory, the weakest cross section in this case is the nanostructure base. The force applied to the NW tip can be defined as:

$$F = \frac{M_{max}}{l} \quad (1),$$

where M_{max} - is the maximum bending moment corresponding to the elastic strain, l - NW length. M_{max} can be found using the following expression:

$$M_{max} = S \cdot \sigma \quad (2),$$

where S - elastic section modulus, and σ - elastic stress. For the beam having circular cross section the section modulus can be calculated as $S = \frac{\pi r^3}{4}$, where r - is the rod radius**.** According to the Hooke's law:

$$\sigma = \varepsilon \cdot E \tag{3},$$

where E - Young's modulus. Summing up equations (1)-(3) we arrive at dependence of the force F on the strain and geometry of the NW:

$$F = \frac{\pi r^3}{4l} E \cdot \varepsilon \tag{4}.$$

Within the strength of materials theory, deflection of the rod in this case is given by:

$$b = \frac{F \cdot l^3}{3E \cdot I} \tag{5},$$

where I - second moment of area, for circular cross section $I = \frac{\pi r^4}{4}$**.** To verify applicability of the equations above we modeled experimental data from [5], where, the author studied a deflection of a 50 nm thick and 1.5 μm long inclined GaP NW under bending by the tip of an atomic force microscopy (AFM) probe. Schematic of the experiment is presented in **Figure S15**a. Within the experiment, the author applied specified force to the probe and measured dependence of the NW deflection on the point of the force application x (see Figure S15a). The results of the experiment are presented in Figure S15b. These curves were modeled using equation (5), where the Young's modulus value of GaP E = 10^{11} Pa [5]. The modeled curves are depicted in Figure S15b together with the experimental data. As can be seen, theoretical data fits well the experiment allowing us to estimate analytically the forces evolved by the cells.

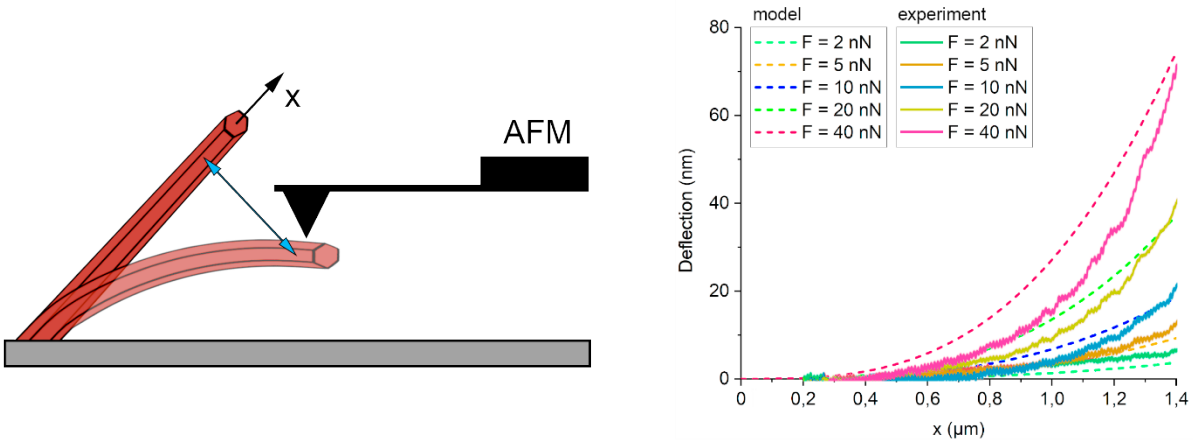

Figure S15. The forces and deflections provided by the cell. a) schematic of the NW bending experiment carried out in [5] with AFM tip; b) bending profile of GaP NW, experimental data taken from [5] and original modeling results.

REFERENCES

[1] Hällström W, Lexholm M, Suyatin DB, Hammarin G, Hessman D, Samuelson L, et al. Fifteen-piconewton force detection from neural growth cones using nanowire arrays. Nano Lett 2010;10:782–7.

[2] Sharov V, Alekseev P, Fedorov V, Mukhin I. Raman Spectroscopy of gallium phosphide nanowires under 5% elastic strain. The European Conference on Lasers and Electro-Optics, Optica Publishing Group; 2021, p. ce_p_3.

[3] Sharov VA, Bolshakov AD, Fedorov V V, Bruyere S, Cirlin GE, Alekseev PA, et al. Deep-subwavelength raman imaging of the strained GaP nanowires. The Journal of Physical Chemistry C 2020;124:14054–60.

[4] Chen Y, An X, Liao X. Mechanical behaviors of nanowires. Appl Phys Rev 2017;4.

[5] Bespalova K. Experimental measurement of Young's modulus of gallium phosphide nanowires by atomic force microscopy 2018. Lappeenranta University of Technology (https://lutpub.lut.fi/handle/10024/157333)